

7-2013

# Magnetic and Structural Properties of Rapidly Quenched Tetragonal $Mn_{3-x}Ga$ Nanostructures

Yung Huh

*University of Nebraska-Lincoln, yung.huh@sdstate.edu*

Parashu Kharel

*University of Nebraska at Lincoln, pkharel2@unl.edu*

Shah R. Valloppilly

*University of Nebraska-Lincoln, svalloppilly2@unl.edu*

E. Krage

*University of Nebraska-Lincoln*

Ralph Skomski

*University of Nebraska at Lincoln, rskomski2@unl.edu*

*See next page for additional authors*

Follow this and additional works at: <http://digitalcommons.unl.edu/physicsskomski>

---

Huh, Yung; Kharel, Parashu; Valloppilly, Shah R.; Krage, E.; Skomski, Ralph; Shield, Jeffrey E.; and Sellmyer, David J., "Magnetic and Structural Properties of Rapidly Quenched Tetragonal  $Mn_{3-x}Ga$  Nanostructures" (2013). *Ralph Skomski Publications*. 78.  
<http://digitalcommons.unl.edu/physicsskomski/78>

This Article is brought to you for free and open access by the Research Papers in Physics and Astronomy at DigitalCommons@University of Nebraska - Lincoln. It has been accepted for inclusion in Ralph Skomski Publications by an authorized administrator of DigitalCommons@University of Nebraska - Lincoln.

---

**Authors**

Yung Huh, Parashu Kharel, Shah R. Valloppilly, E. Krage, Ralph Skomski, Jeffrey E. Shield, and David J. Sellmyer

# Magnetic and Structural Properties of Rapidly Quenched Tetragonal $\text{Mn}_{3-x}\text{Ga}$ Nanostructures

Y. Huh<sup>1,2</sup>, P. Kharel<sup>1,3</sup>, V. R. Shah<sup>1</sup>, E. Krage<sup>1,2</sup>, R. Skomski<sup>1,3</sup>, J. E. Shield<sup>1,4</sup>, and D. J. Sellmyer<sup>1,3</sup>

<sup>1</sup>Nebraska Center for Materials and Nanoscience, University of Nebraska, Lincoln, NE 68588 USA

<sup>2</sup>Department of Physics, South Dakota State University, Brookings, SD 57007 USA

<sup>3</sup>Department of Physics and Astronomy, University of Nebraska, Lincoln, NE 68588 USA

<sup>4</sup>Department of Mechanical and Materials Engineering, University of Nebraska, Lincoln, NE 68588 USA

**Nanostructured  $\text{Mn}_{3-x}\text{Ga}$  ribbons with  $x = 0, 0.4, 0.9$  and  $1.1$  were prepared using arc-melting, melt-spinning and annealing. As-spun samples crystallized into hexagonal  $\text{D0}_{19}$  and cubic  $\text{L2}_1$  Heusler crystal structures based on the concentration of Mn in  $\text{Mn}_{3-x}\text{Ga}$ . Upon vacuum-annealing the samples at  $450^\circ\text{C}$  for about 50 hours, both the hexagonal and cubic structures transformed into a tetragonal  $\text{D0}_{22}$  structure. High-temperature x-ray diffraction and high-temperature magnetometry showed that the samples with low Mn content ( $\text{Mn}_{1.9}\text{Ga}$  and  $\text{Mn}_{2.1}\text{Ga}$ ) retain their tetragonal structure up to 850 K but the samples with high Mn concentrations ( $\text{Mn}_{2.6}\text{Ga}$  and  $\text{Mn}_{3.0}\text{Ga}$ ) undergo a structural phase transition from tetragonal to hexagonal phases around 800 K. The magnetic properties of  $\text{Mn}_{3-x}\text{Ga}$  ribbons were very sensitive to Mn concentration, where the magnetization and anisotropy energy increased and the coercivity decreased as  $x$  increased from 0 to 1.1. Although the Curie temperatures of  $\text{Mn}_{2.6}\text{Ga}$  and  $\text{Mn}_{3.0}\text{Ga}$  samples could not be determined because of the structural phase transition, the Curie temperature decreased with increasing  $x$  in  $\text{Mn}_{3-x}\text{Ga}$ . The maximum magnetization of  $57\text{ emu/g}$  ( $300\text{ emu/cm}^3$ ) and the coercivity of  $6.5\text{ kOe}$  were measured in the  $\text{Mn}_{1.9}\text{Ga}$  and  $\text{Mn}_{3.0}\text{Ga}$  ribbons, respectively.**

**Index Terms**—Magnetic anisotropy, melt-spun ribbons, permanent magnet, spintronic device.

## I. INTRODUCTION

**M**ATERIALS with high magnetic anisotropy and Curie temperature well above room temperature have potential for a range of applications including high-density recording, nonvolatile memory and permanent-magnet materials [1]–[3]. Some of these materials in thin films show high perpendicular anisotropy and also a large value of spin polarization [4]. This unique combination of materials properties is useful in developing novel spintronic devices including nonvolatile spin-transfer torque (STT) memory [3]. A manganese-based ferromagnetic material  $\text{Mn}_{3-x}\text{Ga}$  ( $0 \leq x \leq 1$ ) in the tetragonal  $\text{D0}_{22}$  structure is one such material that exhibits a combination of various technologically important properties including low magnetization, high spin polarization, high perpendicular anisotropy, high coercivity and high Curie temperature well above room temperature [5]. An important feature of this material is that the structural and magnetic properties can be tuned with the value of  $x$  to fit a specific practical application. Other interesting magnetic properties of the  $\text{Mn}_{3-x}\text{Ga}$  system are as follows: 1) Theoretical calculations predict that  $\text{Mn}_3\text{Ga}$  in cubic structure exhibits half-metallic electronic band structure with antiferromagnetic spin order [6]. This new class of material, although not realized experimentally yet, is believed to be useful in improving the performance of a spin-polarized scanning tunneling microscope (SPSTEM) because the antiferromagnetic tip does not produce any stray field [7]. 2)  $\text{Mn}_{3-x}\text{Ga}$  ( $0 \leq x \leq 1$ ) in the hexagonal structure

is a strong room-temperature antiferromagnet and has potential for an exchange-bias spin-valve sensor [8]. 3)  $\text{Mn}_{3-x}\text{Ga}$  ( $1.4 \leq x \leq 2$ ) in the tetragonal  $\text{L1}_0$  structure shows very high coercivity  $H_c$  and also high magnetic anisotropy  $K$  ( $H_c = 42\text{ kOe}$  and  $K = 22.9\text{ Mergs/cm}^3$  in  $\text{Mn}_{1.5}\text{Ga}$  films) at room temperature [9]. These interesting properties of multifunctional character have stimulated renewed interest in investigating various properties of this material [10], [11].

Although  $\text{Mn}_{3-x}\text{Ga}$  shows relatively low magnetization and energy product, the high values of  $H_c$  and  $K$  observed in its tetragonal  $\text{L1}_0$  and  $\text{D0}_{22}$  structures are promising and could be useful in developing nonrare-earth-element based hard-soft exchange coupled nanocomposite permanent magnet with  $\text{Mn}_{3-x}\text{Ga}$  serving as the hard magnetic component. Exchange coupling between the hard and soft phases can be realized only in nanocomposites. Therefore, it is important to understand the magnetic properties of this material in nanoparticle or nanostructured-ribbon form. In this report, we present our experimental investigation on the structural and magnetic properties of  $\text{Mn}_{3-x}\text{Ga}$  ( $0 \leq x \leq 1.1$ ) nanostructured ribbons. We have synthesized  $\text{Mn}_{3-x}\text{Ga}$  ribbons in various structures including cubic  $\text{L2}_1$ , hexagonal  $\text{D0}_{19}$ , tetragonal  $\text{L1}_0$  and tetragonal  $\text{D0}_{22}$  depending on elemental compositions and annealing conditions. However, we focus only on the tetragonal  $\text{D0}_{22}$  structure in this work.

## II. EXPERIMENTAL METHODS

$\text{Mn}_{3-x}\text{Ga}$  ( $x = 0, 0.4, 0.9$  and  $1.1$ ) nanostructured ribbons were prepared using arc-melting, melt-spinning and annealing. The arc-melting process, which produces  $\text{Mn}_{3-x}\text{Ga}$  ingots from the respective metal pieces, was carried out on a water-cooled Cu hearth in a highly pure argon environment. The intended elemental compositions were estimated from the starting weights of Mn and Ga metal pieces. In order to

Manuscript received October 26, 2012; revised January 03, 2013; accepted January 27, 2013. Date of current version July 15, 2013. Corresponding author: Y. Huh (e-mail: yung.huh@sdstate.edu).

Color versions of one or more of the figures in this paper are available online at <http://ieeexplore.ieee.org>.

Digital Object Identifier 10.1109/TMAG.2013.2244856

produce nanostructured ribbons, a molten mixture formed by melting a  $\text{Mn}_{3-x}\text{Ga}$  ingot was ejected onto the surface of a rotating copper wheel where it rapidly solidified into ribbons. The ribbons are about 1 mm wide and 1  $\mu\text{m}$  thick. In order to obtain the intended tetragonal  $\text{D}_{022}$  structure, the ribbons were annealed in a tubular vacuum furnace (base pressure  $\sim 10^{-7}$  Torr) at 450  $^\circ\text{C}$  for about 50 hours. This is a clear advantage of rapidly quenched nanostructure, as the annealing time required to form the tetragonal phase is a lot shorter than previously reported two to three weeks of annealing for an arc-melted ingot [11]. The elemental compositions of the samples were confirmed using energy dispersive x-ray (EDX) spectroscopy (JOEL SEM). The compositions were close to the initially estimated values within an error of 0.1 at. %. The room-temperature structural properties of the samples were studied using x-ray diffraction (XRD) in a Rigaku x-ray diffractometer and the temperature-dependent structural properties were studied using a Bruker AXS D8 Discover, equipped with an Anton Paar domed hot stage (DHS 906), diffractometer. A Quantum Design SQUID magnetometer and a physical properties measurement system (PPMS) were used to investigate the magnetic properties.

### III. RESULTS AND DISCUSSION

#### A. Structural Properties

$\text{Mn}_{3-x}\text{Ga}$  alloys show a number of crystal structures depending on elemental compositions and annealing conditions. Most arc-melted bulk samples and thin films are previously reported to have either hexagonal  $\text{D}_{019}$  or tetragonal  $\text{D}_{022}$  structures [5], [11], [12]. Von Hans-George reported in 1965 that  $\text{Mn}_{75}\text{Ga}_{25}$  (corresponding to  $\text{Mn}_3\text{Ga}$ ) could exist in face-centered-cubic structure but this phase has not been confirmed experimentally before this work [5], [11], [13]. We observed an interesting structural transformation from hexagonal to cubic with increasing Mn content in the rapidly quenched  $\text{Mn}_{3-x}\text{Ga}$  nanostructured ribbons. As-spun  $\text{Mn}_{2.1}\text{Ga}$  is pure hexagonal but the structure begins to transform into cubic as  $x$  in  $\text{Mn}_{3-x}\text{Ga}$  decreases below 0.5 with  $\text{Mn}_3\text{Ga}$  being cubic  $\text{L}_{21}$  Heusler structure, Fig. 1(a). All the as-spun samples, however, crystallized into the tetragonal structure after they were annealed in a vacuum furnace ( $\sim 10^{-7}$  Torr) at 450  $^\circ\text{C}$  for about 50 hours, Fig. 1(b). Both lattice parameters  $c$  and  $a$  change linearly with the change in Mn concentration in  $\text{Mn}_{3-x}\text{Ga}$ , where  $c$  increases by about 1.5% and  $a$  decreases by about 0.4% as  $x$  changes from 0 to 1.1. All ribbons are polycrystalline with no noticeable texture and do not show any preferential orientation according to XRD analysis.

In order to understand the high-temperature structural properties including structural phase transition, we have performed x-ray powder diffraction of annealed  $\text{Mn}_{2.1}\text{Ga}$  and  $\text{Mn}_{3.0}\text{Ga}$  (both tetragonal at room temperature) ribbons in the temperature range between 300 and 850 K. As shown in Fig. 2(a), the  $\text{Mn}_{2.1}\text{Ga}$  unit cell expands almost uniformly in both  $a$  and  $c$  directions until the temperature reaches 740 K. As temperature exceeds 740 K, the unit cell expands about five times faster in  $c$  direction than below 740 K, but the rate of expansion in  $a$  direction remains the same.

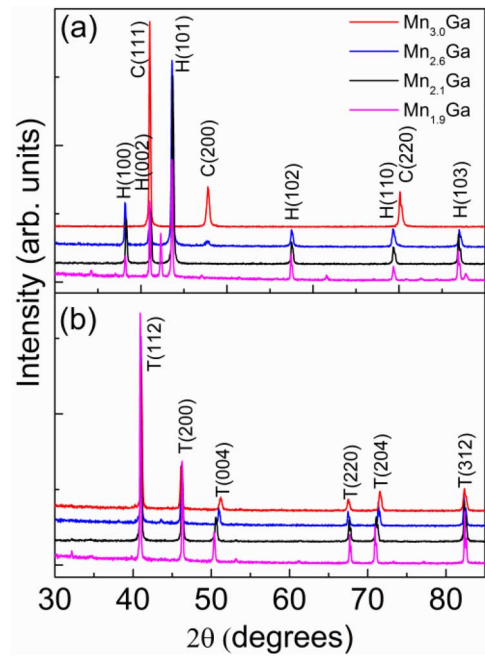


Fig. 1. Room-temperature  $\text{Cu } K_{\alpha}$  x-ray diffraction patterns of (a) as-spun, and (b) annealed  $\text{Mn}_{3-x}\text{Ga}$  ribbons. C, H, and T refer to the cubic  $\text{L}_{21}$ , hexagonal  $\text{D}_{019}$ , and tetragonal  $\text{D}_{022}$  crystal structures respectively.

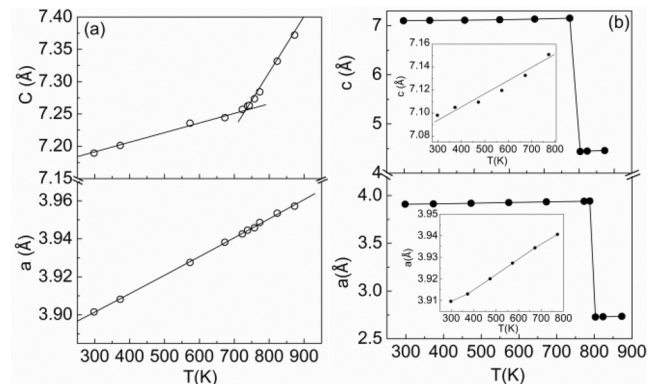


Fig. 2. Temperature dependence of  $c$ - and  $a$ -axes lattice parameters of annealed (a)  $\text{Mn}_{2.1}\text{Ga}$ , and (b)  $\text{Mn}_{3.0}\text{Ga}$  ribbons. The insets in (b) show the thermal expansion of the  $c$  and  $a$  between 300 K and 800 K.

$\text{Mn}_{2.1}\text{Ga}$  maintains its tetragonal structure up to our highest measurement temperature of 850 K. On the other hand, although both  $a$  and  $c$  lattice parameters of  $\text{Mn}_{3.0}\text{Ga}$  show a uniform expansion from room temperature to 800 K, this compound undergoes an abrupt structural phase transition from tetragonal to hexagonal as temperature exceeds 800 K. As  $\text{Mn}_{2.1}\text{Ga}$  was cooled back to room temperature from 850 K, it retained its initial tetragonal structure. However, the structural phase transition of  $\text{Mn}_{3.0}\text{Ga}$  was irreversible and it remained hexagonal even after it was cooled to room temperature from 850 K. The effect of structural phase transition on the magnetic properties of  $\text{Mn}_{3-x}\text{Ga}$  nanostructures will be discussed below.

#### B. Magnetic Properties

The magnetic field dependence of magnetizations of  $\text{Mn}_{3-x}\text{Ga}$  ribbons in tetragonal structure measured at room temperature is shown in Fig. 3. All the samples show wide  $M(H)$  hys-

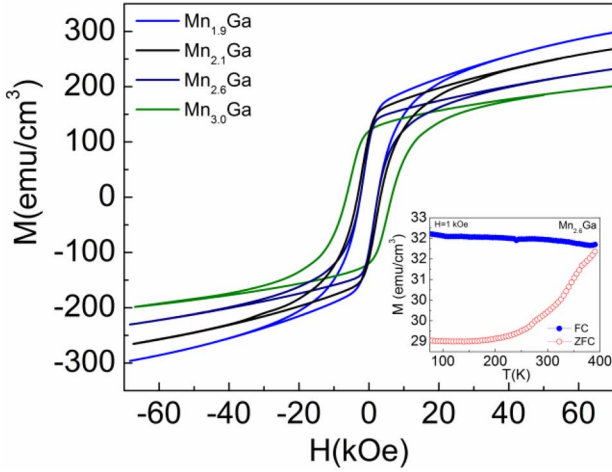


Fig. 3. Magnetization,  $M(H)$ , of tetragonal  $Mn_{3-x}Ga$  ribbons measured at room temperature. The inset shows the ZFC (open) and FC (solid) curves of tetragonal  $Mn_{2.6}Ga$  ribbon at 1 kOe.

TABLE I  
MAGNETIC PROPERTIES OF TETRAGONAL  $Mn_{3-x}Ga$  RIBBONS

Samples	$M_{70\text{ kOe}}$ ( $\text{emu}/\text{cm}^3$ )	$H_c$ (kOe)	$K$ ( $\text{Merg}/\text{cm}^3$ )	$T_c$ (K)
$Mn_{3.0}Ga$	201	6.5	1.8	799 <sup>a</sup>
$Mn_{2.6}Ga$	233	4.0	2.1	796 <sup>a</sup>
$Mn_{2.1}Ga$	271	3.5	3.0	735
$Mn_{1.9}Ga$	300	2.5	3.6	702

<sup>a</sup>Structural Phase Transition Temperature.

teresis loops with the high field ( $H = 70$  kOe) magnetization and coercivity showing a substantial change with the change in  $x$  in  $Mn_{3-x}Ga$ .

As listed in Table I, the high-field magnetization linearly increases from  $201 \text{ emu}/\text{cm}^3$  ( $1.2 \mu_B/\text{unit cell}$ ) to  $300 \text{ emu}/\text{cm}^3$  ( $1.8 \mu_B/\text{unit cell}$ ) as  $x$  in  $Mn_{3-x}Ga$  increases from 0 to 1.1 but coercivity decreases from 6.5 kOe to 2.5 kOe for the same change in the value of  $x$ . The high-field value of magnetization ( $1.2 \mu_B/\text{unit cell}$ ) for  $Mn_{3.0}Ga$  is little smaller than the total magnetic moment per unit cell ( $1.702 \mu_B/\text{unit cell}$ ) predicted by the first-principles calculation [11], which is expected because the  $M(H)$  loops are not saturated even at 70 kOe. This also suggests that  $Mn_{3-x}Ga$  ribbons have substantial magnetic anisotropy as polycrystalline samples of highly anisotropic magnetic materials typically display unsaturated  $M(H)$  loops. The anisotropy energy,  $K$ , is highly sensitive to the concentration of Mn in  $Mn_{3-x}Ga$  ribbons. The  $K$  values increase almost linearly from  $1.8 \text{ Merg}/\text{cm}^3$  for  $Mn_{3.0}Ga$  to  $3.6 \text{ Merg}/\text{cm}^3$  for  $Mn_{1.9}Ga$  (see Table I). The anisotropy energy was calculated using the approach-to-saturation method, where the high-field data were fitted to  $M = M_0(1 - A/H^2) + \chi H$ ;  $A = 4K^2/15M_0^2$ . The parameters  $M_0$ ,  $A$  and  $\chi$  are the spontaneous magnetization, a constant that depends on  $K$  and the high field susceptibility, respectively [14].

Although Mn has a large value of atomic magnetic moment, most manganese compounds show relatively low saturation magnetization because of the competing ferro- and antiferromagnetic couplings between Mn moments located at different crystallographic sites. In hexagonal  $D0_{22}$

$Mn_{3.0}Ga$ , the local magnetic moment of Mn at 2b position ( $Mn_{II} = -3.069 \mu_B$ ) is directed opposite to that of the Mn at 4d position ( $Mn_{III} = 2.416 \mu_B$ ) resulting in a small value of total magnetic moment per unit cell [11], [15]. Since the total moment is parallel to  $Mn_{III}$ , Mn vacancies in 2b sites should increase the net magnetization. Although the observed increase in magnetization with increasing number of Mn vacancies in  $Mn_{3-x}Ga$  is consistent with this argument, the linear but small increase of saturation magnetization with increasing  $x$  does not agree and needs different explanation. Our experimental results, the increase in magnetization of  $Mn_{3-x}Ga$  ribbons with increasing  $x$ , are in good agreement with the proposed preferential loss of Mn from both 2b and 4d sites [11].

The temperature dependence of magnetization,  $M(T)$ , from 10 K to 400 K was measured under zero-field-cooled (ZFC) and field-cooled (FC) conditions at 1 kOe applied field. For the ZFC measurement, the ribbons were cooled from room temperature to 10 K without applying any magnetic field. After applying a magnetic field of 1 kOe at 10 K, magnetizations were recorded as the samples were heated. For the FC measurement, the samples were cooled from 400 to 10 K at the same field and magnetizations were measured while heating. All  $Mn_{3-x}Ga$  ribbons show a qualitatively similar  $M(T)$  behavior, where magnetizations are irreversible between ZFC and FC measurements with the inflection points above room temperature. However, the divergence between the ZFC and FC curves measured at 10 K becomes more pronounced as  $x$  in  $Mn_{3-x}Ga$  increases from 0 to 1.1. The ZFC/FC curves of  $Mn_{2.6}Ga$  ribbon are shown as the inset of Fig. 3. In contrast to our results, the ZFC/FC data recorded in the  $Mn_{3.0}Ga$  and  $Mn_{2.1}Ga$  bulk samples show spin-glass like magnetic transitions at 164 and at 145 K, respectively [11]. The splitting between the ZFC and FC curves observed in our samples could be explained as the consequence of the frustrated spin structures caused by the competing ferromagnetic and antiferromagnetic interactions between Mn moments located at different crystallographic sites of  $Mn_{3-x}Ga$  nanostructures.

The temperature dependence of magnetizations of  $Mn_{3-x}Ga$  ribbons above 300 K is shown in Fig. 4. Magnetizations were measured at 1 kOe as temperature increased from 300 to 850 K and as temperature decreased from 850 K to 300 K. The magnetizations of the samples with low Mn concentrations ( $Mn_{1.9}Ga$  and  $Mn_{2.1}Ga$ ) show different temperature dependence than those of the samples with high Mn content ( $Mn_{2.6}Ga$  and  $Mn_{3.0}Ga$ ), although they show similar  $M(T)$  behavior below room temperature. For  $Mn_{1.9}Ga$  and  $Mn_{2.1}Ga$  ribbons, there exist magnetic phase transitions from ferrimagnetic to paramagnetic phases as temperature increases above their Curie temperatures (see Fig. 4). High temperature  $M(T)$  curves do not show any thermal hysteresis between heating and cooling, but the magnetizations during cooling are larger than heating (see the inset of Fig. 4). Since the applied field of 1 kOe is not sufficient to saturate the magnetization below the Curie temperature, there could be magnetic domain rearrangements as the samples cool through Curie temperature at a magnetic field resulting in an increase in the magnetization. On the other hand, the magnetizations in  $Mn_{2.6}Ga$  and  $Mn_{3.0}Ga$  ribbons increase with increasing temperature but undergo a sharp irreversible decrease as the

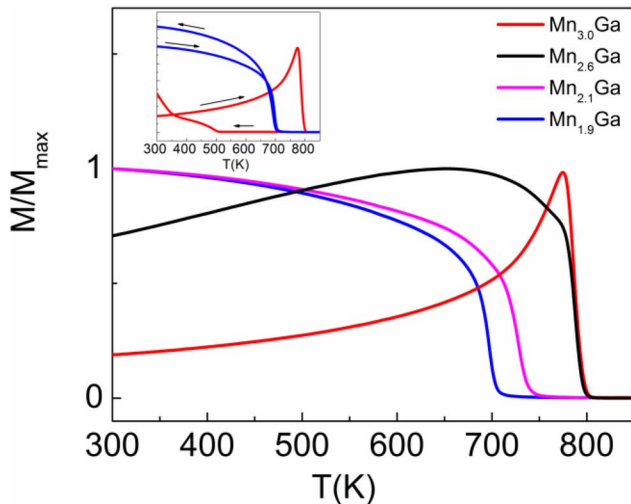


Fig. 4. Magnetization,  $M(T)$ , of tetragonal  $Mn_{3-x}Ga$  ribbons during heating from room temperature to 850 K. Inset shows  $M(T)$  curves of  $Mn_{1.9}Ga$  and  $Mn_{3.0}Ga$  ribbons during both heating and cooling. The vertical scale of the inset is also  $M/M_{max}$ , where  $M_{max}$  is the maximum value of magnetization in the corresponding heating curves.

samples pass through structural phase transition from a ferrimagnetic tetragonal phase to a paramagnetic hexagonal phase around 800 K (see Fig. 4 and its inset). This phase transition is consistent with the x-ray diffraction studies as explained above. However, as temperature decreases, the magnetization starts increasing as the weak ferrimagnetic order appears below 500 K, which is consistent with the previous report [16]. As shown in Table I, the Curie temperatures for  $Mn_{1.9}Ga$  and  $Mn_{2.1}Ga$  are respectively 702 K and 735 K but the Curie temperatures for  $Mn_{2.6}Ga$  and  $Mn_{3.0}Ga$  could not be determined because of the structural phase transition that occurred before the Curie temperature was reached. Table I summarizes the high-field magnetization, coercivity, anisotropy energy and Curie temperature of these samples.

#### IV. CONCLUSION

Nanostructured  $Mn_{3-x}Ga$  ( $x = 0, 0.4, 0.9$  and  $1.1$ ) ribbons were prepared using arc melting, melt spinning and annealing. As-spun ribbons showed an interesting structural transformation from hexagonal  $D0_{19}$  to cubic  $L2_1$  Heusler structures as the value of  $x$  in  $Mn_{3-x}Ga$  decreased below 0.5. Regardless of crystal structures in as-spun ribbons, all samples transformed into tetragonal  $D0_{22}$  structure after vacuum annealing. Samples in tetragonal structure showed a ferrimagnetic spin order at room temperature with high coercivity, high anisotropy energy and Curie temperature well above room temperature. The high-field magnetization increased by a factor of about two as the value of  $x$  in  $Mn_{3-x}Ga$  increased from 0 to 1.1. The increase in magnetization in  $Mn_{3-x}Ga$  ribbons with the increase in  $x$  is explained as the consequence of a reduction of magnetic compensation in the ferrimagnetic unit cell due to the preferential loss of Mn atoms from both the 2b and 4d crystallographic sites.

The observed high values of coercivity (6.5 kOe in  $Mn_{3.0}Ga$ ) and magnetic anisotropy (3.6 Mergs/cm<sup>3</sup> in  $Mn_{1.9}Ga$ ) shows that the material has potential for spintronic devices such as spin transfer torque devices due to its small magnetization, high spin polarization, high Curie temperature and moderate coercivity. The magnetic properties of  $Mn_{3-x}Ga$  ribbons can be further improved with suitable external impurity doping.

#### ACKNOWLEDGMENT

This work was supported by DOE (DMR-0820521) (D.J.S., R.S.), NSF MRSEC (NSF-DMR-0820521) (P.K., Y.H., E.K.), ARPA-E (DE-AR0000046) (J.E.S.), and NCMN. Y. Huh would like to thank the colleagues of Prof. Sellmyer's research group at UNL for their generous hospitality during his recent sabbatical leave.

#### REFERENCES

- [1] A. Perumal, Y. K. Takahashi, T. O. Seki, and K. Hono, "Particulate structure of  $L1_0$  ordered ultrathin FePt films for perpendicular recording," *Appl. Phys. Lett.*, vol. 92, pp. 132508–3, 2008.
- [2] J. M. D. Coey, "Hard magnetic materials: A perspective," *IEEE Trans. Magn.*, vol. 47, pp. 4671–4681, 2011.
- [3] R. Sbiaa, H. Meng, and S. N. Piramanayagam, "Materials with perpendicular magnetic anisotropy for magnetic random access memory," *Phys. Status Solidi RRL*, vol. 5, pp. 413–419, 2011.
- [4] P. Kharel, P. Thapa, P. Lukashev, R. F. Sabirianov, E. Y. Tsymlal, D. J. Sellmyer, and B. Nadgorny, "Transport spin polarization of high curie temperature MnBi films," *Phys. Rev. B*, vol. 83, pp. 024415–6, 2011.
- [5] H. Kurt, K. Rode, M. Venkatesan, P. Stamenov, and J. M. D. Coey, "High spin polarization in epitaxial films of ferromagnetic  $Mn_3Ga$ ," *Phys. Rev. B*, vol. 83, pp. 020405–4(R), 2011.
- [6] S. Wurmehl, H. C. Kandpal, G. H. Fecher, and C. Felser, "Valence electron rules for prediction of half metallic compensated-ferrimagnetic behavior of Heusler compounds with complete spin polarization," *J. Phys.: Condens. Mater.*, vol. 18, pp. 6171–6181, 2006.
- [7] H. van Leuken and R. A. de Groot, "Half metallic antiferromagnets," *Phys. Rev. Lett.*, vol. 74, pp. 1171–1173, 1995.
- [8] B. Dieny, V. S. Speriosu, S. S. P. Parkin, B. A. Gurney, D. R. Wilhoit, and D. Mauri, "Giant magnetoresistance in soft ferromagnetic multilayers," *Phys. Rev. B*, vol. 43, pp. 1297–1300, 1991.
- [9] L. Zhu, S. Nie, K. Meng, D. Pan, J. Zhao, and H. Zheng, "Multifunctional  $L1_0 - Mn_{1.5}Ga$  films with ultrahigh coercivity, giant perpendicular magnetocrystalline anisotropy and large magnetic energy product," *Adv. Mater.*, vol. 24, pp. 4547–4551, 2012.
- [10] H. Kurt, K. Rode, M. Venkatesan, P. Stamenov, and J. M. D. Coey, " $Mn_{3-x}Ga$  ( $0 \leq x \leq 1$ ): Multifunctional thin film materials for spintronics and magnetic recording," *Phys. Status Solidi*, vol. 248, pp. 2338–2344, 2011.
- [11] J. Winterlik, B. Balke, G. H. Fecher, C. Felser, M. C. M. Alves, F. Bernardi, and J. Morais, "Structural, electronic, and magnetic properties of tetragonal  $Mn_{3-x}Ga$ : Experiments and first-principles calculations," *Phys. Rev. B*, vol. 77, pp. 054406–12, 2008.
- [12] T. J. Nummy, S. P. Bennett, T. Cardinal, and D. Heiman, "Large coercivity in nanostructured rare-earth-free  $Mn_xGa$  films," *Appl. Phys. Lett.*, vol. 99, pp. 252506–3, 2011.
- [13] H.-G. Meißner and K. Schubert, "Zum Aufbau einiger zu  $Tb^{5-}$ -Ga homologer und quasihomologer Systeme," *Z. Metallkd.*, vol. 56, pp. 523–530, 1965.
- [14] G. Hadjipanayis and D. J. Sellmyer, "Rare-earth-rich metallic glasses. I. Magnetic hysteresis," *Phys. Rev. B*, vol. 23, pp. 3349–3354, 1981.
- [15] S. Mizukami, T. Kubota, F. Wu, X. Zhang, and T. Miyazaki, "Composition dependence of magnetic properties in perpendicularly magnetized epitaxial thin films of Mn-Ga alloys," *Phys. Rev. B*, vol. 85, pp. 014416–6, 2012.
- [16] H. Niida, T. Hiro, and Y. Nakagawa, "Magnetic properties and crystal distortion of hexagonal  $Mn_3Ga$ ," *J. Phys. Soc. Jpn.*, vol. 52, no. 5, pp. 1512–1514, May 1983.